Lithofacies Control on Reservoir Quality of the Viola Limestone in Southwest Kansas and Unsupervised Machine Learning Approach of Seismic Attributes Facies-Classification

ABDELMONEAM E. RAEF,[1] MATTHEW W. TOTTEN,[1] ARIA LINARES,[1] and ARASH KAMARI[1]

Abstract—The hydrocarbon development of the Viola Limestone in southern Kansas, USA, has encountered challenges, regarding the development of a robust data-based model of the reservoir-quality controls. The legacy understanding that hydrocarbon entrapment and reservoir-quality are controlled by structure, has resulted in less than optimal drilling results. In this study, an integration of petrographic and geophysical well-logs analyses established the main reservoir quality control as dolomitization-induced porosity. The dolomitization control is supported by comparing best-fit trends on density-porosity well log values with typical model-trends of limestone and dolomite density-porosity. Furthermore, this study presents unsupervised artificial neural network (ANN) classification, based on five seismic attributes (instantaneous frequency, energy, band width, absorption quality factor, seismic amplitude), that comes in agreement with Ca–Mg ratio and the observed sonic transit time (DT log) variation with dolomitization/porosity increase. The hydrocarbon reservoir facies identified by the attributes classification explains the drilling results, with high accuracy/match to facies class centers, and can be used effectively in other settings. The integration, of multi-scale multi-data analysis and modeling, has provided a solid understanding of the reservoir-quality control and distribution. This study can be considered as a reliable platform for placing future infill wells in the study area, to lower the risk of drilling dry holes.

Key words: Porosity, unsupervised neural networks, viola formation, seismic attributes.

1. Introduction

Petroleum producing areas within the mid-continent region, USA, discovered in the first half of the 1900s often ignored the potential of deeper formations once hydrocarbons were discovered in shallower zones. This is particularly true in areas of western Kansas where Mississippian-aged production was established, primarily because of the concern of controlling the active water-drive reservoirs before modern cementing technologies were developed. The Ordovician-aged Viola Limestone is one of the overlooked formations.

This certainly holds true for Clark and Comanche counties of Kansas, where Mississippian-aged production commenced in the 1930s and continues today. As late as the 1970s, Viola production west of Kiowa and Comanche counties of Kansas was not expected due to a perceived lack of seal (Rascoe 1971). The unexpected discovery of the Box Ranch field in 1988 established Viola production in Comanche County, which initiated a Viola play in this part of Kansas. The subsequent discovery in 2000 of Viola pay in the Herd Field in central Comanche county further sparked interest in the Viola as a viable exploration target (Richardson 2013).

Development of the Herd field demonstrated that Viola production was not controlled by simple structure, but by selective preservation of dolomite porosity underneath an erosional unconformity beneath the overlying Maquoketa Shale (Richardson 2013). Recognition of these "paleotopographic" traps was expected to occur with thinning of the Maquoketa above the trap (Fig. 1). A thicker section of Maquoketa was deposited in areas where the dolomitic facies were eroded away, resulting in poor reservoir quality. This overlooked formation has posed challenges as to developing Morrison and Morrison Northeast fields of Clark County, Kansas. Those challenges arose from the lack of understanding the main controls on reservoir quality and entrapment setting, (Raef et al. 2017; Linares 2016).

Consequently, 3D seismic surveys were conducted to explore for these ideal conditions favorable for Viola production. One such survey in easternmost

[1] Department of Geology, Kansas State University, Manhattan, KS 66506, USA. E-mail: abraef@ksu.edu
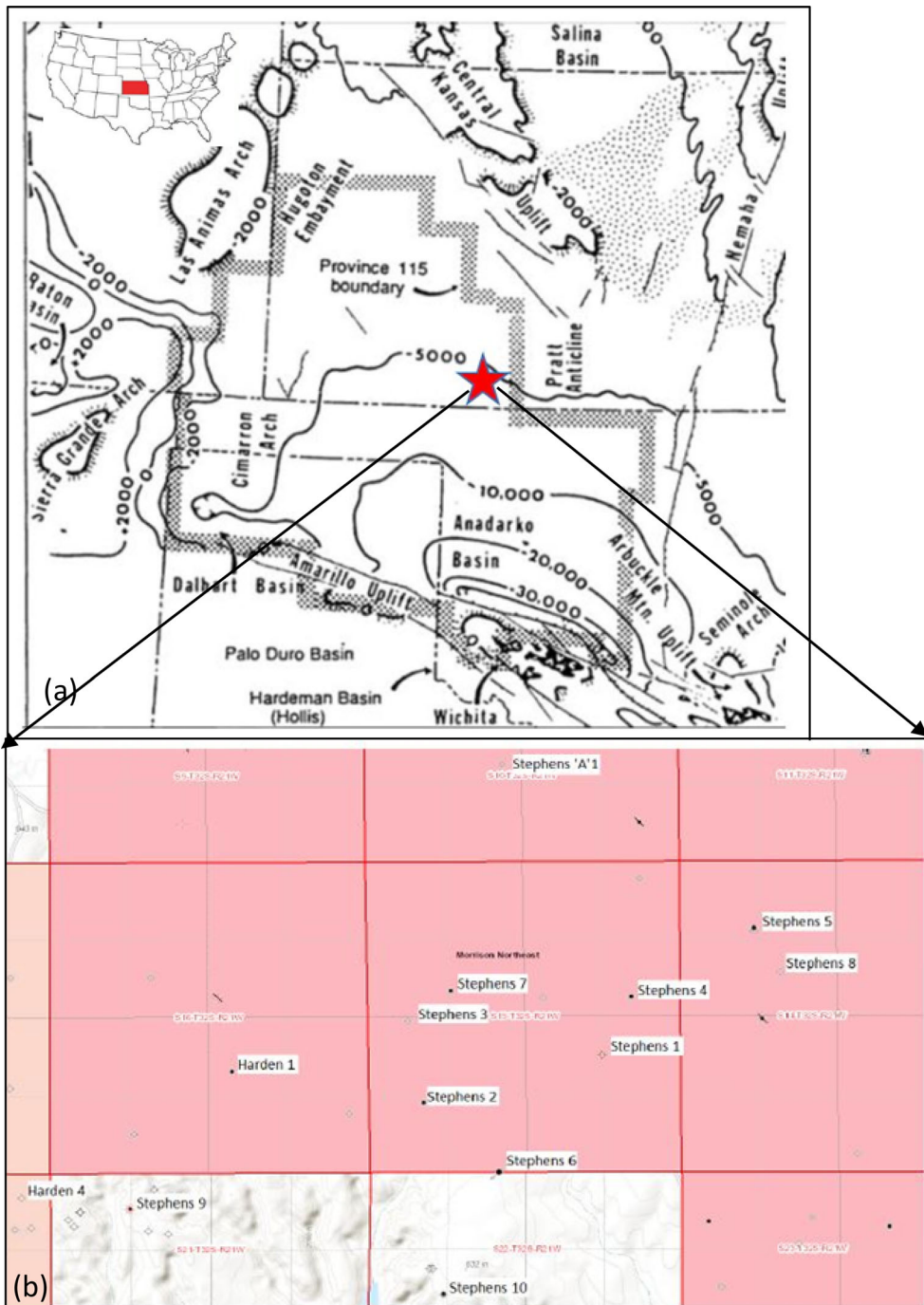
Figure 1
a Depth-to-basement map and structural provinces of south central mid-continent, **b** location map of Morrison NE field of Clark County, south-central Kansas

Clark County led to the opening of the Morrison Northeast Field by Coral Coast Petroleum in 2012. A total of 13 wells were drilled, of which 7 are still producing. Development of the field was hindered by the high heterogeneity of the Viola reservoir properties. Reinterpretation of the 3D dataset by Raef

et al. (2017) reported seismic facies associated with producing wells based upon seismic attributes. These facies were reported to be associated with distinct reservoir lithofacies that contained the necessary conditions for hydrocarbon production.

The objective of this research was to expand the description of the lithofacies beyond Raef et al. (2017), using petrographic and petrophysical methods, to better predict reservoir conditions in the Viola Limestone. A further objective was to better understand the linkage between seismic facies variation in relation to reservoir quality of the different Viola lithofacies.

A workflow to recognize zones with higher productivity combining seismic, well log analyses, and detailed rock description is proposed. The proposed workflow should aid in identifying productive Viola facies using 3D seismic, and reduce the number of dry holes during field development.

2. Geological Setting and Petroleum System

The study area for this research is the Middle Ordovician-aged (470–440 Mya) Viola limestone formation found in the Morrison Northeast Field of Clark County, south-central Kansas. The Viola Limestone Formation is a carbonate reservoir that is widely exposed throughout Texas, Oklahoma, Nebraska, Missouri and Kansas, yielding moderate production rates of oil and gas throughout its course (Carlson and Newell 1997). In most of this region, the production rate of the Viola is mostly controlled by the geologic structure, but in south-central Kansas much of the Viola limestone's reservoir quality is determined by stratigraphic and petrographic aspects that are a combination of the rock's depositional environment and diagenetic alterations (Richardson 2013; Syed et al. 2010).

Stratigraphic traps in the Viola Limestone include the Herd, Bird East and Box Ranch oil fields in Comanche County, (Fig. 1), collectively produced as much as 2.2 million barrels of oil (BO) and 9.7 billion cubic feet of gas (BCFG) (Richardson 2013). The Morrison NE Field, which is the subject of this study has produced over 200,000 barrels since its discovery in 2012.

The Maquoketa limestone is a difficult to recognize but important unit with regard to Viola limestone production in the Morrison NE field. This dense limestone serves as the seal above the Viola limestone in the study area. The Maquoketa is a cream to light gray, dense limestone with no visible porosity and an average thickness of about 20–25 ft within the study area. The Maquoketa thins over paleotopographic highs of the Viola, and thickens in the lows. This dense non-porous rock makes an excellent seal for the petroleum system in the area (Richardson 2013).

The Morrison NE Field was discovered using a 3D seismic survey, focusing on an isochrone map of the Maquoketa to identify "thinning" of this formation, and preservation of the Viola "A" zone. Development of the field was hindered by the unpredictable relationship between the Maquoketa thinning and reservoir properties, resulting in several dry holes.

The Viola limestone was deposited in the middle Ordovician period in a warm tropical marine setting. The Viola varies between a fossiliferous limestone, and a medium to coarse crystalline vuggy dolomite, often containing scattered chert, with a total thickness of about 175–200 ft within the study area. It is informally divided into four distinct facies, delineated as the "A" through "D" zones. A stratigraphic column of the Viola within the study area is displayed in Fig. 2.

Vugs within the Viola "A" zone result in excellent porosity/permeability, which makes it an outstanding hydrocarbon reservoir rock (Goebel 1968). The Viola sits below an erosional unconformity representing about 20 Ma of subaerial exposure, contributing to the formation of vugs that give the Viola "A" such good porosity and permeability. In some areas the "A" and sometimes also the "B" zone are eroded away, resulting in a lack of reservoir conditions in non-productive limestone facies. Hence, the key to establishing development-model is determining where the Viola "A" and/or "B" zone are preserved in a structurally favorable setting. An example of the resulting paleotopographic trap within the Viola as the result of this erosional unconformity in the analogous Herd Field is shown in Fig. 3.
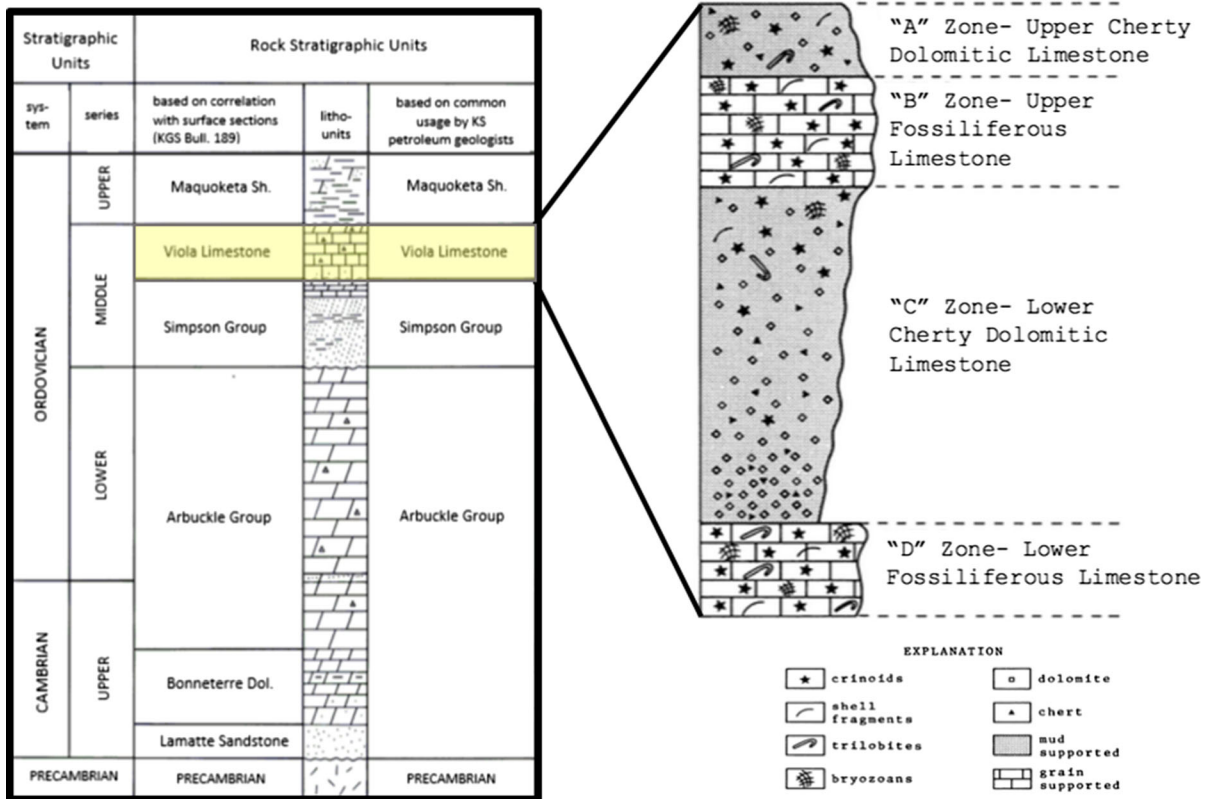
Figure 2
Stratigraphic column showing formations of interest in the study area and the four distinct lithofacies within the Viola (modified after Cole 1975)
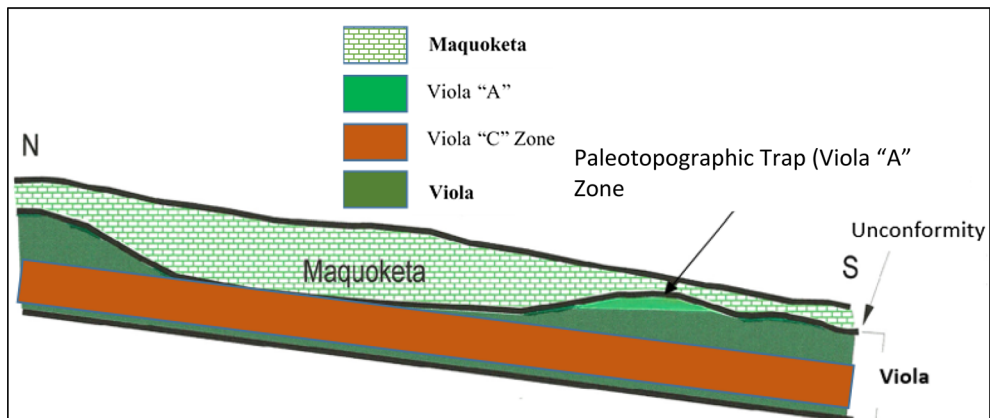

Figure 3
Idealized cross section showing paleotopographic traps within the Viola of the Herd Field, Comanche County, Kansas. The Herd Field is approximately fifteen miles east of the study area (modified after Richardson 2013)

A re-interpretation of the seismic volume focusing on attribute analyses was conducted by Reaf et al. (2017) and Vohs (2016). Combining the amplitude attribute on the top of the Viola with an Instantaneous Frequency thin-bed indicator successfully separated the producing wells from the unsuccessful wells in

Table 1

Thin-section descriptions, Ca/Mg ratios based upon SEM-EDS peaks (averaged to account for EDS inaccuracies), and ImageJ calculations of thin-section porosity

Well	Thin section description	Ca/Mg	Thin section porosity
Stephens 4 Producer	Fossiliferous packstone/grainstone dolostone; some iron oxide staining on dolomite; Minor chert, porosity visible along fractures in packstone; more fracture fabric-supported porosity present	3	20.5
Harden 1 Producer	Grainstone dominant; allochems include forams and bryozoan; pyritic; dolomite more anhedral rhombic with intercrystalline porosity; minor glauconite; some packstone present with good vuggy and fracture porosity	5	15.1
Stephens 6 Producer	Dolomite with equant crystals dominant; Ooids and intraclasts more prevalent with interparticle porosity; presence of bryozoan noted; much more fossiliferouspackstone-moremud-rich wackestone/packstone present; possible anhydrite present; minor packstone with muddy edges; pyrite present; minor chert present	4	13.2
Stephens 8 Dry hole	Intrasparite limestone dominant; sucrosic subhedral dolostone; minor staining; very pyritic; minor clay; minor chert; some interparticle/intercrystalline and fracture porosity; minor intercrystalline porosity on dolostone	30	5.7
Stephens 9 Dry hole	Packstone/grainstone dominant with ostracod, brach, and ooids; some presence of chert; not as much subhedral dolomite present; interooid porosity and minor fracture porosity along oolitic limestone; lots of hematite/siderite staining; some oil stain; very minor interparticle porosity	80	3.0
Stephens 3 Dry hole	Packstone dominant; prominent grey shale; minor dolomite present with subhedral rhombs; chert much more prevalent; prominent pyrite present; Very low porosity overall	160	3.9

the field. The thin bed tuning of the instantaneous frequency was reported to be enhanced by the presence of hydrocarbons, but is largely controlled by the thickness of the reservoir facies and the lowered amplitude of the high porosity reservoir facies.

3. Petrography and Well-Logs Facies

The close agreement between the seismic facies and reservoir lithofacies reported in Raef et al. (2017) encouraged us to further investigate the petrologic controls affecting both. Core was not available on any of the wells in the field, hence we looked at drill cuttings that were lagged back to pertinent drilling depths using ROP logs. This was aided by several points where drilling was stopped to circulate for samples. These depths gave the best confidence that we were selecting the actual samples from a specific drilling depth.

Well cuttings were vacuum impregnated with blue-dyed epoxy, mounted on standard thin-section slides, ground to 30 micron thickness, and polished. Images in plane light were uploaded into ImageJ software (Linares, 2016) which calculates the area of

the image represented by the blue epoxy-filled porosity. These data are listed in Table 1. As expected, the productive wells have higher porosity values. A diagnostic characteristic of the reservoir lithofacies is the presence of dolomite.

The polished sections were further examined under a scanning electron microscope (SEM). X-ray spectra were collected at relatively low magnification under SEM (Fig. 4) using an energy dispersive detector (EDS), which represent averages of the major element chemistry in the field of view. The mineralogy varied primarily between dolomite and calcite, with minor chert, as determined by petrographic microscope, which was confirmed by Ca-to-Mg ratios as determined by characteristic peak heights of the EDS spectra. Admittedly these are semi-quantitative, however the large difference between dolomite and calcite make these a useful indicator of each rock type. These values are included in Table 1. The reservoir lithofacies in the producing wells, based upon the Ca-to-Mg ratio (and the thin-section description), are dolomitic, and have the highest porosity. The non-productive lithofacies are limestone, with very poor porosities.
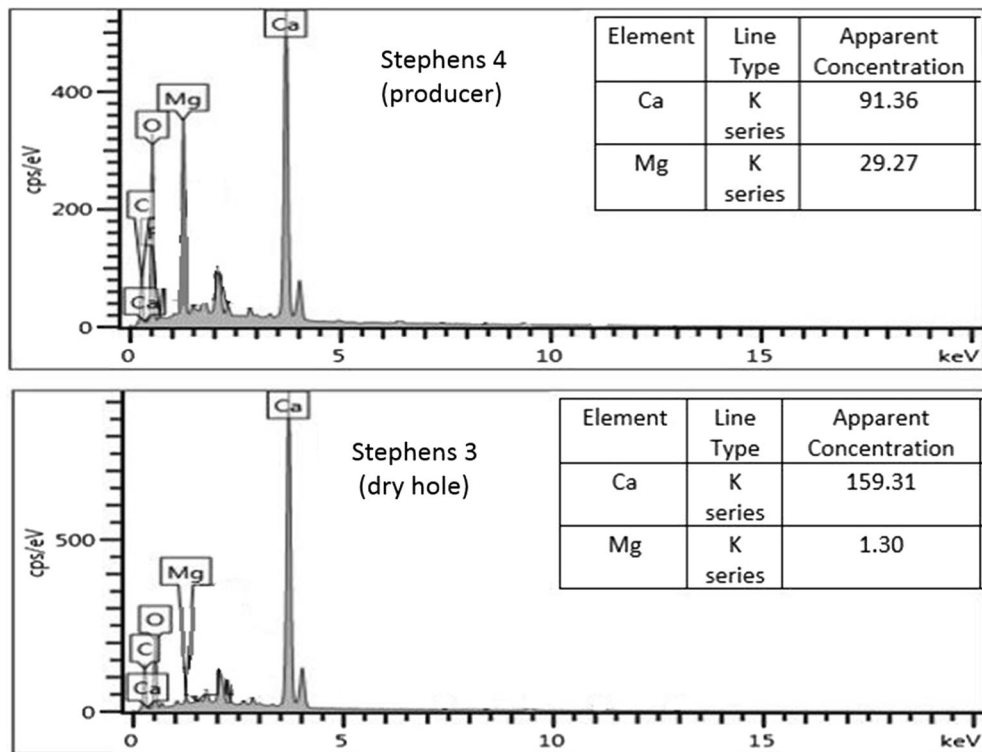
Figure 4
SEM–EDS spectra from a dolomitic lithofacies (Stephens 4) and a limestone lithofacies (Stephens3). They differ in the ratio of the Ca to the Mg peak

The lithofacies recognized petrographically also are identifiable by their distinctive well log characteristics. Figure 5 is a crossplot of bulk density versus neutron porosity for three producing wells and two dry holes. Note that only the producers have values that plot in the high porosity, low bulk density regions of the graph. Also plotted on the same figure is the relationship between dolomitization, based upon Ca–Mg ratios, and porosity (as determined by thin section). Figure 5 also shows calculated trends of varying mineral composition and associated fluid content within the pore space. Note that the producing wells plot in a trend parallel to oil-bearing dolomite (solid black line). In contrast, the non-productive wells vary similarly to brine-bearing limestone. This validates the agreement between thin-section petrography, EDS chemistry, and well log characteristics in separating the productive reservoir lithofacies from the non-productive lithofacies. Furthermore, the best-fit trend (black dotted line) to the

productive reservoir facies is parallel and in proximity to a typical oil-bearing dolomite trend (black solid line). In contrast, the best-fit trend (blue dotted line) of the non-productive facies is parallel to and midway in between the typical brine-bearing limestone trend and brine-bearing dolomite trend (blue solid line). These relationships of the best-fit trends of the productive facies and non-productive facies strongly suggest dolomitization control on porosity and in turn on reservoir quality.

In a similar fashion, Fig. 6 shows the separation between productive and non-productive lithofacies using a neutron porosity and sonic transit-time log crossplot. The dolomitic productive facies follows a trend similar to a modeled 85% dolomite-15% chert line, in agreement to observed thin-section descriptions and the association of cherty dolomite facies for the upper Viola formation (Bornemann and Doveton 1983). Most importantly, the higher porosity values follow an expected decreasing seismic amplitude for
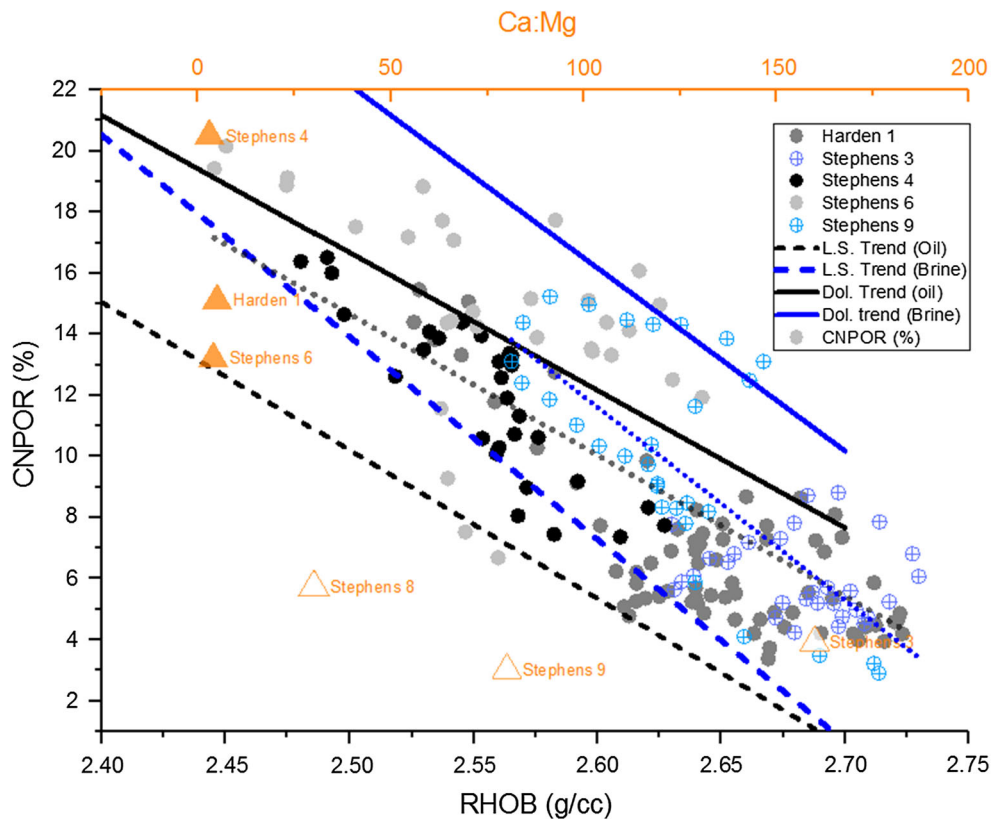
Figure 5
Cross-plots of bulk density (RHOB log)-Compensated Neutron porosity (CNPOR) for oil wells in shades of grey circles and brine wells in tones of blue; several trends density-porosity for different litho-facies is plotted; solid blue line (brine-bearing dolomite), solid black line (oil bearing dolomite), dashed blue line (brine-bearing limestone), dashed black (oil-bearing limestone), dotted black line (best-fit trend for oil-producers modelled as dolomite lithofacies), and dotted blue line (best-fit trend for brine-bearing Viola wells modelled as limestone lithofacies)

the top of the Viola horizon. This finding have strong potential to help identify the productive dolomitic lithofacies utilizing the 3D seismic data. The typical porosity transient time trends and the data best-fit curves are based on the model published by Raiga-Clemenceau et al. (1988).

4. Seismic Attributes and Supervised ANN Facies Classification

The proliferation of seismic attributes utilization in seismic reservoir characterization has been enforced with the adoption of machine learning and well-logs facies calibration for hydrocarbon plays in the stages of exploration and development (e.g., Hadavand et al. 2018; Raef et al. 2017; Ansari et al.

2015; Ohl and Raef 2014; Riedel et al. 2013; Chopra and Marfurt 2008; Hard and Balch 2000; Gastaldi et al. 1997; Schmitt 1999; Chen and Sidney 1997). A comprehensive historical prospective of seismic attributes has been reported by Chopra and Marfurt (2005). In this study, we have analyzed the petrographic results, well-logs facies cross-plots, and lithology typical porosity-density and porosity-sonic trends with the aim of understanding main controls on reservoir quality and establish ties to seismic attributes facies. Given the thin thickness of the pay-zone of the viola, based on well-logs facies, and the expected decrease in the peak-tracking Viola-horizon seismic amplitude, a seismic facies defined by thin-layer responsive attributes, namely, (higher) thin-bed indicator and instantaneous frequency, and (lower) seismic amplitudes (Fig. 7) became evident as the
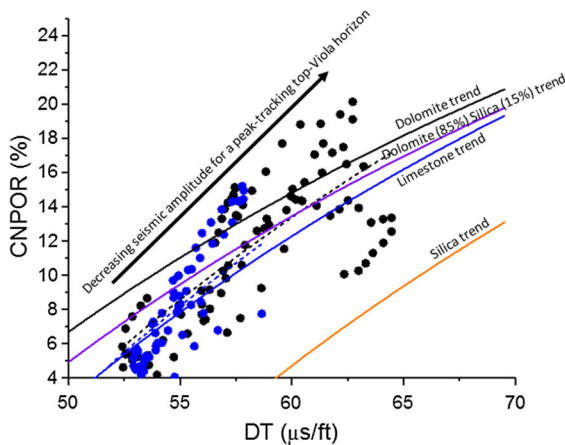
Figure 6
Cross-plots of sonic transient time (DT-log) versus Compensated Neutron Porosity for oil-producers (black circles) and typical lithology trends of DT-porosity and the effect of Chert occurrence (15%) on the Dolomite trend; the fitted (dashed black) trend of oil-producing well is in better agreement with the modeled 85% Dolomite-15% Chert at higher porosities

seismic facies that corresponds with better reservoir lithofacies. The mixed oil and dry-hole development drilling results of the Stephens Ranch lease, provided an opportunity to test our hypothesis, regarding the relevance of the seismic facies to reservoir quality lithofacies (Figs. 6a, b, 7). Oil wells cluster at higher instantaneous frequency and thin-bed indicator (Fig. 7a) with lower peak amplitude values (Fig. 7a, b). Both the thin-bed indicator and instantaneous frequency attributes were the root-mean-square (RMS) values in a window of 20 ms; OpendTect (6.2) is the seismic interpretation software used for the seismic attributes extraction and the time-window RMS-computation. Based on the complex trace concept (Taner et al. 1979), the instantaneous frequency is defined the derivative of the instantaneous phase. The thin bed indicator is the difference between the instantaneous frequency and envelope weighted frequency, (Iturrarán-Viveros 2012)

Our choice of a machine learning model for seismic facies classification is unsupervised vector quantizer artificial neural networks, UVQ-ANN, (e.g., Gersho and Gray 1992; Kostina 2017). UVQ-ANN application to seismic facies classification has been utilized in many case studies around the world (e.g., Huang et al. 1990; Saggaf et al. 2003; Coléou et al. 2003). According to a comparison of various

neural networks in seismic facies classification presented in Ross and Cole (2017), unsupervised network has been applied effectively to macro- and meso-scale depositional facies classification. Recent work by Roden et al. (Roden et al. 2015) presents a case study of determining reservoir-scale properties based on an unsupervised neural network. Assigning a meaningful interpretation of an unsupervised neural network output of classes need to be well-anchored or calibrated to well-logs facies and/or core-based petrographic and petrophysical analyses, and regional depositional and stratigraphic knowledge of the target rock formation. To this end, in this study we train and apply a UVQ-ANN to classify, into three classes, the seismic waveform of the top horizon of the Viola-formation (Fig. 8a) and build an understanding of the resulting seismic classes (facies) in terms of petro-physical and lithofacies description based on well-logs facies models and analytical "dolomitization criteria" Ca–Mg ratio (Figs. 6, 7). Both the match to class-centers values and the separation of the class-centers in the hyperspace of the input five-attributes evidence the quality of the waveform classification.

The class centers values for the five attributes (seismic horizon amplitude, instantaneous frequency, energy, bandwidth, absorption quality factor) and match values (Table 2) testify for robust classification. The correlation of class distributions (Fig. 8a), strongly suggests the association of Class I facies with reservoir facies, i.e. higher degree of dolomitization as manifested by low Ca-to-Mg ratios for Stephens 4 and 6 and Harden 1 (Fig. 5) and lower amplitude (lower seismic Viola-horizon amplitude (Fig. 7a, b). Class 2 facies is thin-bed facies as evidenced by high values of instantaneous frequency—there are no drilling results available. Class III facies is characterized by high amplitude and in conformance with the drilling results of Stephens 3 and Stephens 8; far less proportions of dolomitization "low-porosity Limestone" brine bearing facies and high seismic Viola-horizon amplitude.

5. Discussion and Conclusions

In this study, a synergistic work flow incorporating multi-scale data of core-sample petrography,
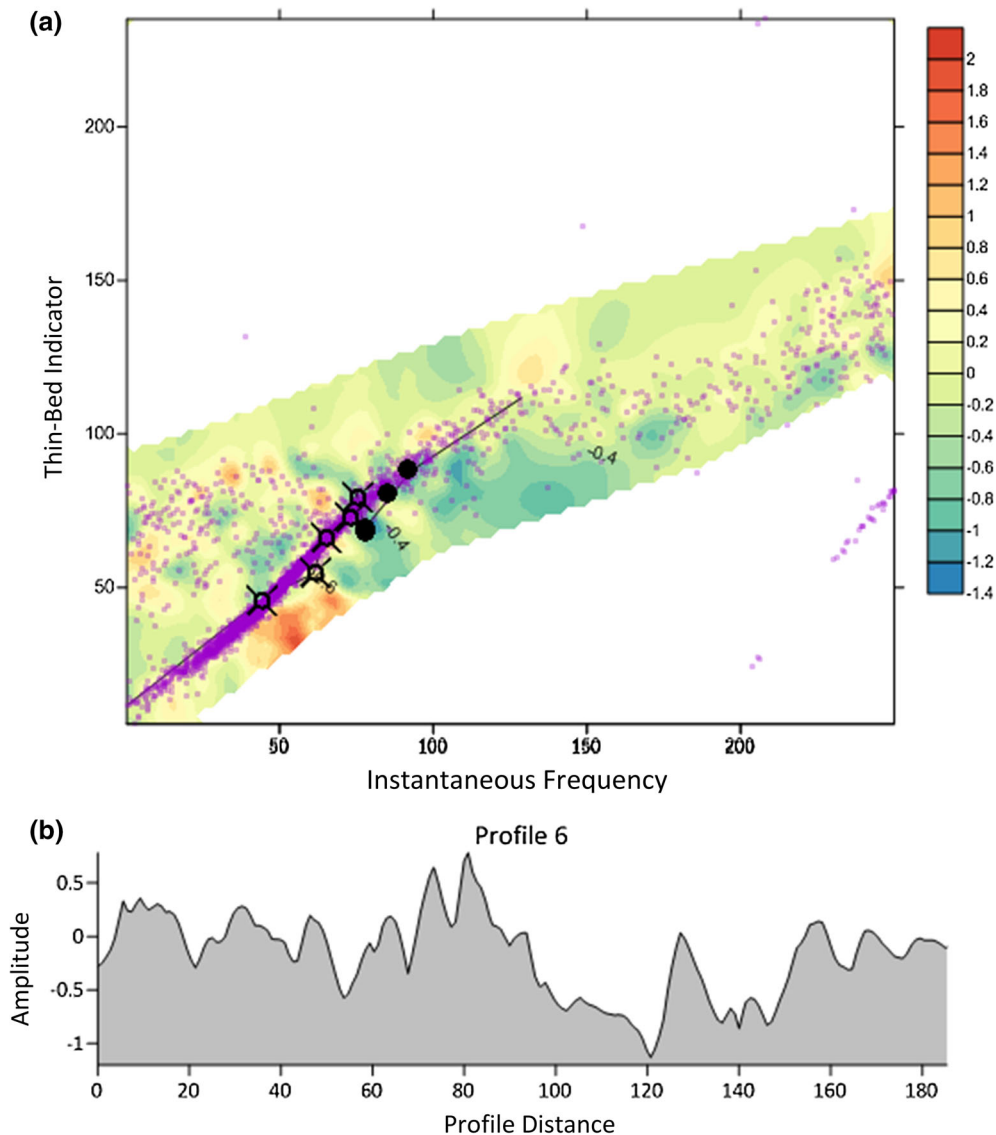
Figure 7
a Three seismic attributes plot; with instantaneous frequency versus thin-bed indictor scatter plot, and seismic amplitude as color overlay; dry-hole wells are separated as higher amplitude (as also evidenced by **a** profile, **b** passing through all wells) and lower values instantaneous frequency and thin-based indicator seismic facies

well-logs data of brine-bearing and oil-bearing wells, and UVQ-ANN based seismic attributes classification, resulted in relationships between best-fit trends of productive and non-productive lithofacies. This result is corroborated by the petrographic analysis and in agreement with an UVQ seismic facies classification based on five seismic attributes. Class I seismic facies (green on Fig. 8a) is in close agreement with drilling results, and is interpreted as the

reservoir-quality facies –higher degree of dolomitization and higher porosity. The low-quality match (blue color-labeled on Fig. 8b), less than 10% of the study area, is to be excluded when utilizing the seismic facies in placing new wells. The distributions of Class I (reservoir facies) and Class III (non-reservoir facies) substantiate the seismic facies reported in a study by Raef et al. (2017).
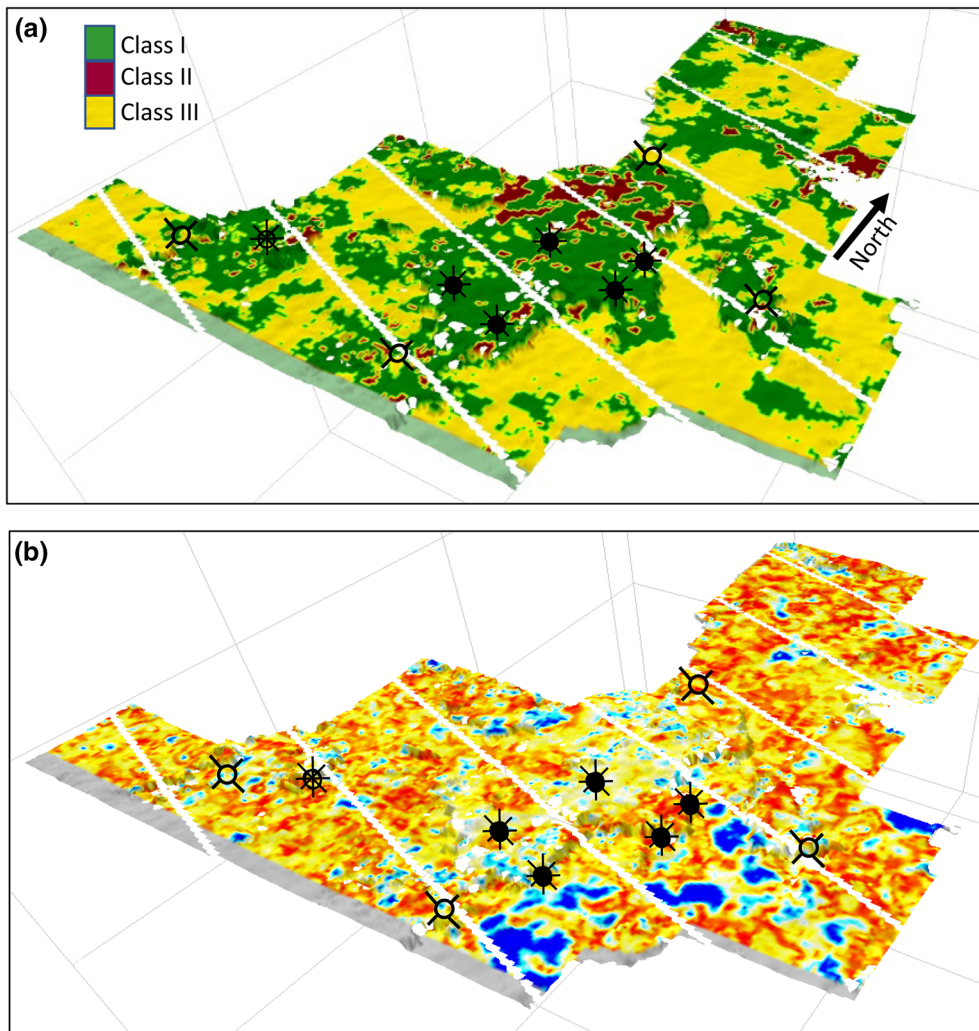
Figure 8

a Unsupervised ANN classification [instantaneous frequency (RMS within a 20 ms window), thin-bed indicator (RMS within a 20 MS window), and seismic horizon amplitude (Viola-top peak amplitude)] map of reservoir (green) and nonreservoir (yellow or brown), **b** seismic amplitude map of Viola horizon (brine-bearing/low-porosity, high amplitude (blue)). Dry holes ⌀ ; Oil wells ✸

The fact that both the Ca-to-Mg ratio and the positions of the best-fit trends of the productive and non-productive facies (Figs. 5, 6) are indicative of dolomitization (with minor chert) control on the reservoir secondary porosity of the Viola. This data and modeling supported observation is in agreement with the findings of Bornnemann and Doveton (1983) study of a south central Kansas Viola Limestone. The results of this work agree with the conclusion of Richardson 2013, in the nearby Herd Field, and suggest that reservoir conditions are only encountered in the Viola when the dolomitized facies are preserved from erosion. These zones are dolomitic, and exhibit porosities sufficient for hydrocarbon production. The higher porosity and lower density of these facies are recognized on log crossplots of porosity curves.

The higher porosities, particularly when filled with hydrocarbon, will slow down seismic velocities, which contributes to the thin-bed tuning as exhibited by instantaneous frequency. Hence, the seismic facies (lower amplitude and higher instantaneous frequency) reported in Raef et al. 2017, is relevant to petrographic and stratigraphic aspects in the reservoir

Table 2

UVQ classification attributes values for class centers, Match, relative importance of attributes in classification

	Class I (Center)	Class II (Center)	Class III (Center)	Attribute− importance (Relative)
Instantaneous Frequency	54.25	**155.5**	52.68	88.7
Band Width	12.95	**47.58**	8.89	94.1
Energy	**2.23**	2.36	**6.04**	99.3
Absorption Quality Factor	**90244**	106118	**197565**	100.0
Seismic Viola horizon Amplitude	0.98	0.23	3.25	46.4
Class-Match	0.90	0.83	0.90	
Color on Fig. 8a				

facies. We propose this to be included in predrill workflow, along with seismic isochrone maps to measure thinning of the overlying Maquoketa, to reduce the risk of drilling of dry holes.

REFERENCES

Ansari, Hamid Reza, Motafakkerfard, Reza, & Riahi, Mohammad Ali. (2015). Probabilistic facies prediction in a carbonate gas reservoir of Iran using stochastic seismic inversion and connectivity algorithm. *Journal of Seismic Exploration, 24*(1), 15–35.

Bornemann, E., & Doveton, J. H. (1983). Lithofacies mapping of viola limestone in South-Central Kansas, based on wireline logs. *Aapg Bulletin-American Association of Petroleum Geologists, 67*(4), 609–623.

Carlson, M.P., &, Newell, K.D. (1997). Stratigraphy and petroleum potential of the Simpson and viola (Ordovician) in Kansas and Nebraska. Simpson and viola groups, in the Southern Midcontinent, 1994 Symposium:Oklahoma Geol. Society, 58–65 pp.

Chen, Q., & Sidney, S. (1997). Seismic attribute technology for reservoir forecasting and monitoring. *The Leading Edge, 16*(5), 445–448.

Chopra, S., & Marfurt, K. J. (2005). Seismic attributes—a historical perspective. *Geophysics, 70*(5), 3SO–28SO.

Chopra, S., & Marfurt, K. J. (2008). Emerging and future trends in seismic attributes. *The Leading Edge, 27*(3), 298–318.

Cole, V. B. (1975). Subsurface ordovician-cambrian rocks in Kansas: Kansas geological survey subsurface. *Geological Series, 2,* 18.

Coléou, T., Poupon, M., & Azbel, K. (2003). Unsupervised seismic facies classification: a review and comparison of techniques and implementation. *The Leading Edge, 22*(10), 942–953.

Gastaldi, C., Biguenet, J. P., & De Pazzis, L. (1997). Reservoir characterization from seismic attributes: an example from the Peciko Field (Indonesia). *The Leading Edge, 16*(3), 263–266.

Gersho, A., & Gray, R. M. (1992). *Vector quantization and signal compression.* New York: Kluwer Academic Publishers.

Goebel, E. D. (1968). Mississippian rocks of western Kansas. *AAPG Bulletin, V, 52,* 1732–1778.

Hadavand, M., Carmichael, P., Dalir, A., Rodriguez, M., Silva, D.F., & Deutsch, C.V. (2018). Integration of 4D seismic in steam-assisted-gravity-drainage reservoir characterization. SPE reservoir evaluation & engineering.

Hart, B. S., & Balch, R. S. (2000). Approaches to defining reservoir physical properties from 3-D seismic attributes with limited well control: an example from the Jurassic Smackover Formation, Alabama. *Geophysics, 65*(2), 368–376.

Huang, K.Y., Chang, W.R., & Yen, H.T. (1990). Self-organizing neural network for picking seismic horizons. In *SEG technical program expanded abstracts 1990* (pp. 313–316). Society of Exploration Geophysicists.

Iturrarán-Viveros, U. (2012). Smooth regression to estimate effective porosity using seismic attributes. *Journal of Applied Geophysics, 76,* 1–12.

Kostina, V. (2017). Data compression with low distortion and finite blocklength. *IEEE Transactions on Information Theory, 63*(7), 4268–4285.

Linares, A. (2016). Petrographic analysis and diagenetic history of the Viola Limestone at Stephens Ranch, in the Morrison Northeast Field of Clark County, Kansas, M.S. Thesis, Kansas State University.

Ohl, D., & Raef, A. (2014). Rock formation characterization for carbon dioxide geosequestration: 3D seismic amplitude and coherency anomalies, and seismic petrophysical facies classification, Wellington and Anson-Bates Fields, Kansas, USA. *Journal of Applied Geophysics, 103,* 221–231.

Raef, A., Totten, M., Vohs, A., & Linares, A. (2017). 3D seismic reflection amplitude and instantaneous frequency attributes in mapping thin hydrocarbon reservoir lithofacies: morrison NE Field and Morrison. *Field, Clark County, KS, Pure and Applied Geophysics, 174,* 4379–4394.

Raiga-Clemenceau, J., Martine, J.P., Nicoletis, S. (1988). The concept of acoustic formation factor for more accurate porosity determination from sonic transit time data. Log Anal., Jan.–Feb., pp. 54–60.

Rascoe, B., Jr. (1971). Western Kansas and western Nebraska; in, future petroleum provinces of the United States–their geology and potential, I. H. Cram, ed.: American Association of Petroleum Geologists, Memoir 15, 1046–1054

Richardson, L.J. (2013) The herd viola trend, Comanche County, Kansas. AAPG search and discovery article #20220.

Riedel, M., Bahk, J. J., Kim, H. S., Scholz, N. A., Yoo, D. G., Kim, W. S., et al. (2013). Seismic facies analyses as aid in regional gas hydrate assessments. Part-II: prediction of reservoir properties, gas hydrate petroleum system analysis, and Monte Carlo simulation. *Marine and Petroleum Geology, 47,* 269–290.

Roden, R., Smith, T., & Sacrey, D. (2015). Geologic pattern recognition from seismic attributes: principal component analysis and self-organizing maps. *Interpretation, 3*(4), SAE83. https://doi.org/10.1190/int-2015-0037.1.

Ross, C. P., & Cole, D. M. (2017). A comparison of popular neural network facies-classification schemes. *The Leading Edge, 36*(4), 340–349.

Saggaf, M. M., Toksöz, M. N., & Marhoon, M. I. (2003). Seismic facies classification and identification by competitive neural networks. *Geophysics, 68*(6), 1984–1999.

Schmitt, D. R. (1999). Seismic attributes for monitoring of a shallow heated heavy oil reservoir: a case study. *Geophysics, 64*(2), 368–377.

Syed, A. A., Clark, W. J., Moore, W. R., & Dribus, J. R. (2010). Diagenesis and reservoir quality: (oilfield review). *Schlumberger, n., 2,* 14–27.

Taner, M. T., Koehler, F., & Sheriff, R. E. (1979). Complex seismic trace analysis. *Geophysics, 44*(6), 1041–1063.

Vohs, A B. (2016). 3D seismic attributes analysis in reservoir characterization: the Morrison NE field & Morrison field, Clark County Kansas, M.S. Thesis, Kansas State University.